Phase behavior of liquid-crystal films exhibiting the surface smectic-*L* phase

C. Y. Chao,[1,2] J. E. Maclennan,[3] J. Z. Pang,[3] S. W. Hui,[4] and J. T. Ho[2]
[1]*Department of Physics, National Central University, Chung-li, Taiwan, Republic of China*
[2]*Department of Physics, State University of New York at Buffalo, Buffalo, New York 14260*
[3]*Department of Physics, University of Colorado, Boulder, Colorado 80309*
[4]*Department of Biophysics, Roswell Park Cancer Institute, Buffalo, New York 14263*
(Received 4 December 1997; revised manuscript received 19 February 1998)

Free-standing smectic films of a liquid crystal exhibiting the hexatic smectic-*L* phase have been studied using electron diffraction and optical textures. The films show a rich phase diagram as a function of thickness and temperature. A possible phase transition within the surface smectic-*L* phase is observed. [S1063-651X(98)08906-5]

PACS number(s): 61.30.Eb, 64.70.Md

Smectic liquid-crystal systems have a rich variety of phases with different types of in-plane two-dimensional order. Among the most interesting are the tilted hexatic phases. These phases have at least quasi-long-range order in the orientation of the six local in-plane bonds and in the direction of the local molecular tilt. They have only short-range in-plane positional order. Tilted hexatic phases can differ from each other in the relation between the local tilt and bond directions. In the hexatic smectic-*I* (Sm-*I*) phase, the tilt direction is locked along one of the local bonds. In the hexatic smectic-*F* (Sm-*F*) phase, the tilt direction is locked halfway between two local bonds, or 30° from each. Several earlier experiments have investigated the transitions among tilted hexatic phases. Dierker and Pindak [1] observed a direct phase transition from the Sm-*I* to the Sm-*F* phase in five-layer films of a liquid-crystal system. This transition is weakly first order, with large pretransitional anomalies. X-ray diffraction in *N*-(4-*n*-heptyloxy-benzylidene)-4-*n*-heptylaniline (7O.7), which does not exhibit hexatic phases in the bulk, revealed the existence of Sm-*F* and Sm-*I* phases in films thinner than approximately 300 and 25 layers, respectively, the occurrence of these phases being sensitive to both temperature and the film thickness [2]. In experiments on the $L_{\beta'}$ phase of a lyotropic liquid crystal, a new smectic-*L* (Sm-*L*) phase, in which the tilt direction is locked at an angle between 0° and 30° from a local bond, was reported [3]. However, although the Sm-*L* symmetry was found in this system, it was unclear whether the phase is hexatic or multicrystalline [3,4]. The transition between the Sm-*I* and Sm-*F* phases has also been investigated theoretically [5,6]. It was found that an intermediate Sm-*L* phase, in which the tilt direction can vary continuously between the Sm-*I* and Sm-*F* configuration, can indeed occur. More recently, modulated textures observed in free-standing films of 5-(4″-hexyl,3′-fluoro-*p*-terphenyl-4-oxy)-pentanoic acid ethyl ester (FTE1) and other materials strongly suggested the existence of a surface Sm-*L* phase [7,8]. Subsequently, electron diffraction in free-standing FTE1 films has provided the structural evidence for an observation of hexatic Sm-*L* order in a thermotropic liquid crystal [9]. Here we report additional electron-diffraction and optical experiments that yield further insight into the phase transitions involving the surface Sm-*L* phase in FTE1.

For the electron-diffraction studies, free-standing FTE1 films 1 mm in diameter were drawn at about 86 °C in the smectic-*C* (Sm-*C*) phase. Electron diffraction was performed in a transmission electron microscope equipped with a pressurized and temperature-controlled sample chamber [10]. The electron-beam diameter was about 5 μm. The photographic detection plane is perpendicular to the incident beam. The typical scattering intensity in reciprocal space for thin films consists of a diffuse cylindrical shell for a liquid phase and of six diffraction rods for a crystalline or hexatic phase. In a tilted phase, the intensity maxima of the diffraction cylinder or rods are displaced away from the detection plane about an axis which depends on the symmetry of the tilted phase [11]. Thus the intensity distribution of the detected electron-diffraction pattern is very sensitive to the symmetry of the tilt order relative to the underlying hexatic bond axes. The diffraction pattern is a uniform diffuse ring for the smectic-*A* phase, six sharper diffuse arcs of equal intensity for the hexatic-*B* phase, and six sharp Bragg spots for the crystal-*B* phase. For tilted phases, additional intensity modulations are present, resulting in a diffuse ring with twofold intensity modulation for the Sm-*C* phase, a pair of strong arcs and two pairs of weak ones for the Sm-*I* phase, and two pairs of weak arcs and a pair of weaker ones for the Sm-*F* phase. In the case of the Sm-*L* phase, the expectation is that the diffraction pattern consists of three pairs of arcs of different intensity, and this has been confirmed qualitatively using computer simulation [12]. The diffraction patterns for the Sm-*C* tilted liquid and all tilted hexatic phases are shown schematically in Fig. 1.

We have studied the structures of films between three and 15 molecular layers thick on successive cooling and heating runs. The behavior is typified by that in a ten-layer film [9] as follows. The diffraction pattern above 81 °C consists of a diffuse ring with a twofold intensity modulation characteristic of oriented Sm-*C* ordering in the probed region. On further cooling, there is a transition at around 81 °C which is characterized by an enhancement of the in-plane positional order on the surfaces while the interior remains in the Sm-*C* phase. Detailed analysis of the intensity scans both radially and around the diffraction circle confirms that the Sm-*I* phase is now present in the outermost layer on either surface with the interior remaining in the Sm-*C* phase [9]. At 76 °C,

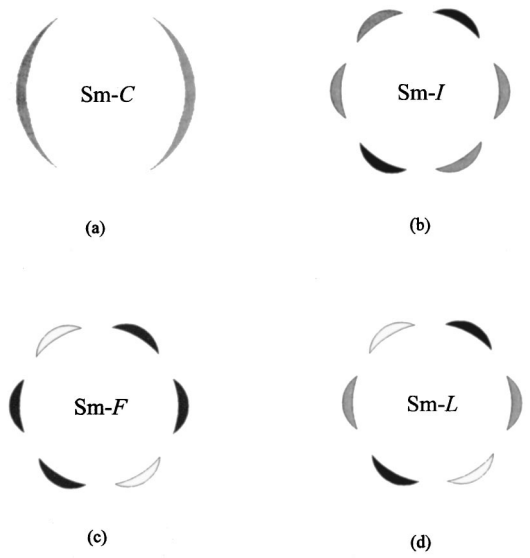

FIG. 1. Electron-diffraction pattern expected in the (a) Sm-*C*, (b) Sm-*I*, (c) Sm-*F*, and (d) Sm-*L* phases.

the film undergoes another surface transition, giving a diffraction pattern shown in Fig. 2, in which two pairs of sharper arcs of different intensity are superimposed on the diffuse Sm-*C* modulated ring. A χ scan around the diffraction circle, as shown in Fig. 3(a), reveals two pairs of uneven hexatic arcs 60° apart and a broad, twofold Sm-*C* background. It has been suggested [4] and confirmed by numerical simulation [12] that the in-plane diffraction pattern of the Sm-*L* phase is characterized by three pairs of arcs of different intensity, as indicated in Fig. 1(d). Thus Fig. 2 signifies the existence of Sm-*L* surface layers on top of the Sm-*C* interior. The absence of a third pair of arcs in the observed Sm-*L* signal is probably due to their diffraction rods being displaced too far away from the detection plane. The χ-scan intensity after subtraction of the interior Sm-*C* contribution is shown as a function of temperature in Fig. 3(b). The gradual shift in the intensity ratio of the two adjacent arcs on cooling suggests a continuous change of the tilt direction of the Sm-*L* surfaces from Sm-*I*-like to Sm-*F*-like, as expected theoretically [5,6]. Our data represent a structural identification of a *hexatic* Sm-*L* phase in a thermotropic liquid-crystal system. At 65 °C, the entire film transforms into the Sm-*F*

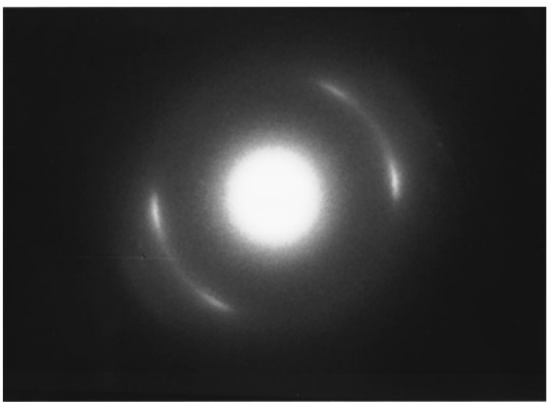

FIG. 2. Electron-diffraction pattern from a ten-layer FTE1 film in the Sm-*L*/Sm-*C* phase at 70.3 °C.

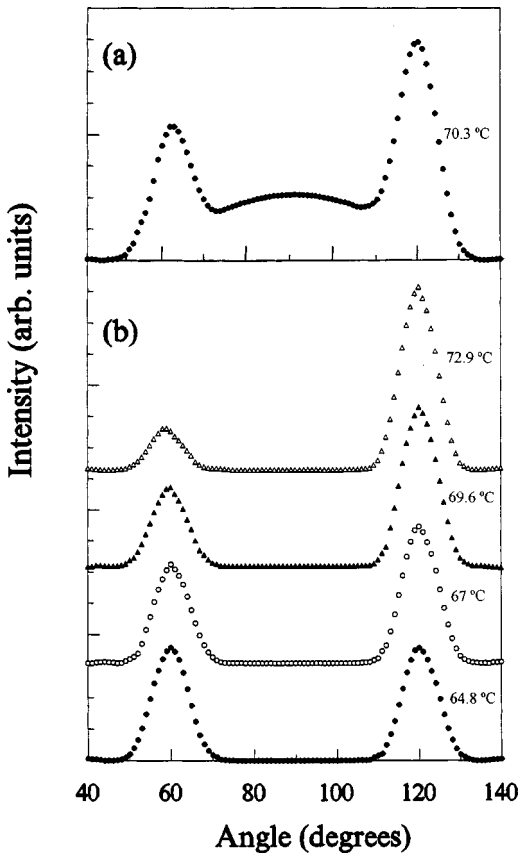

FIG. 3. Diffraction intensity along a χ scan for a ten-layer film (a) at 70.3 °C and (b) at various temperatures after subtraction of the background Sm-*C* contribution. The data in (b) represent the diffraction from the two surface Sm-*L* layers, with the exception of the scan at 64.8 °C, which has been reduced by a numerical factor of about 5 and represents the diffraction from the entire ten-layer Sm-*F* film.

phase, characterized by a diffraction pattern with two pairs of arcs of equal intensity similar to Fig. 1(c). The surface Sm-*L*–Sm-*F* transition appears to be continuous, but it is unclear whether this transition and the interior Sm-*C*–Sm-*F* transition occur at precisely the same temperature.

Unusual stripe textures were observed optically in free-standing FTE1 films using a polarizing microscope with slightly decrossed polarizers, as shown in Fig. 4. Our electron-diffraction structural data directly support the earlier suggestion that the stripes are due to the existence of a surface Sm-*L* phase [3,4]. Uniform stripes separated by sharp, weakly fluctuating walls with Sm-*C*-like director fluctuations in the background were observed optically from 76 °C to 65 °C in FTE1 films of about 15 layers thick, in precisely the same temperature range in which the diffraction pattern in Fig. 2 was observed. The stripe width, which was initially about 3 μm, increased with decreasing temperature. We were able to obtain single-domain diffraction below 73 °C, when the typical stripe width in FTE1 films is larger than the electron-beam diameter of 5 μm [7].

We have conducted numerous temperature runs with electron diffraction, and have compared our results with optical observations of free-standing FTE1 films of thickness from two to 40 layers. The optical phase sequence on heating is shown in Fig. 5 for different layer thicknesses. This phase

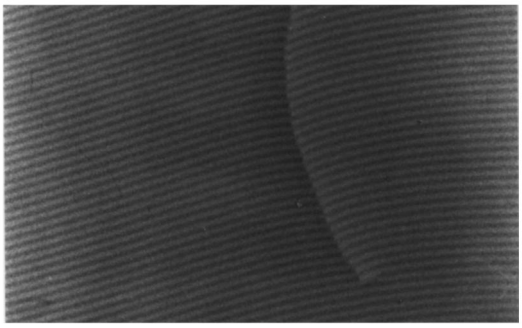

FIG. 4. Typical surface Sm-L stripe textures in a 15-layer FTE1 film viewed in polarized reflected light. Alternating light and dark bands correspond to surface Sm-L domains of opposite chirality. The curved defect is a bend-splay wall that mediates a change in stripe chirality (see Refs. [7,8]). The horizontal dimension of the image is about 250 μm.

diagram for FTE1 thin films is surprisingly rich, since the bulk material only shows a transition from the Sm-C phase to an unknown crystal [8]. Electron diffraction shows that the high-temperature region of the optical phase diagram in which line textures, as shown in Fig. 6(a), were observed corresponds to Sm-I surfaces in the presence of a Sm-C interior (Sm-I/Sm-C). The stripe phase region, as shown in Fig. 6(b), is confirmed to consist of a surface Sm-L phase and an interior Sm-C phase (Sm-L/Sm-C). The low-temperature region below the Sm-L/Sm-C phase where lines are again observed is a Sm-F phase. Optically, the film loses its modulated texture at the transition from the Sm-L/Sm-C to the Sm-F phase. The lowest-temperature region in Fig. 5 has been shown by electron diffraction to consist of novel surface crystal phases with tilted hexatic interiors [9].

Apart from increasing transition temperatures with decreasing thickness, the phase diagram does not change qualitatively from 40 to three layers. Two-layer films are anomalous in that they do not show stripes at any temperature. The same number of phase transitions is observed optically as in thicker films, but since we did not conduct structural studies on two-layer films, the phase identifications are somewhat speculative. We also note that the putative transition from the Sm-F to the Sm-L/Sm-C phase occurs at a much lower temperature than might be expected from the rest of the phase diagram.

An interesting optical observation is that the surface Sm-L region, in which stripes are observed, appears to be divided into two regions, labeled A and B, separated by a

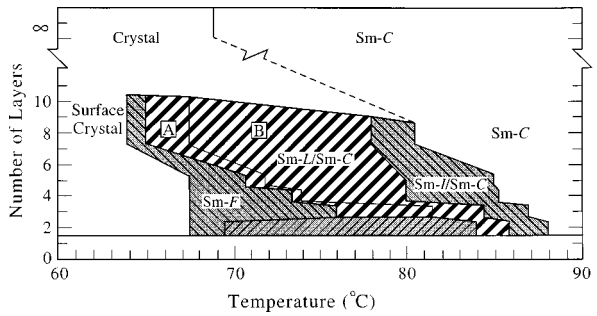

FIG. 5. Phase diagram of FTE1 films of different thicknesses based on optical textures.

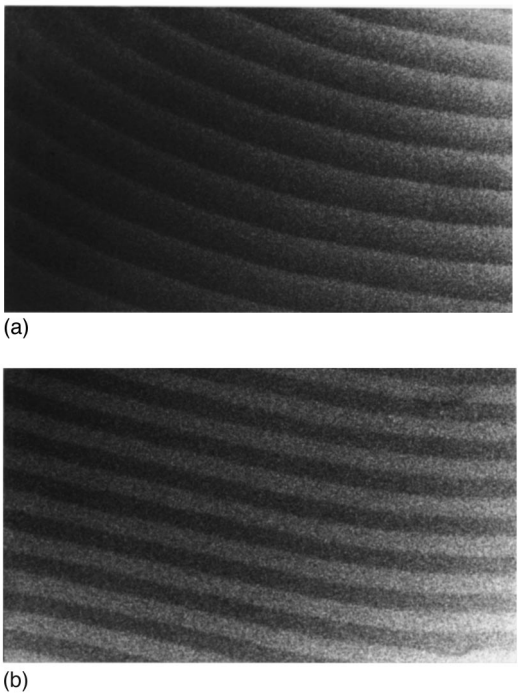

FIG. 6. Typical modulated hexatic textures in a 15-layer FTE1 film viewed in polarized reflected light: (a) sharp lines separating bands with continuously changing intensity characteristic of the surface Sm-I and Sm-F phases, and (b) alternating light and dark stripes corresponding to surface Sm-L domains of opposite chirality. The horizontal dimension of the image is about 125 μm.

textural transition denoted in Fig. 5 by a dashed line. Upon cooling, the stripes disappear momentarily at this transition and then reappear below it, but in regions A and B the film textures are optically indistinguishable. For a ten-layer film,

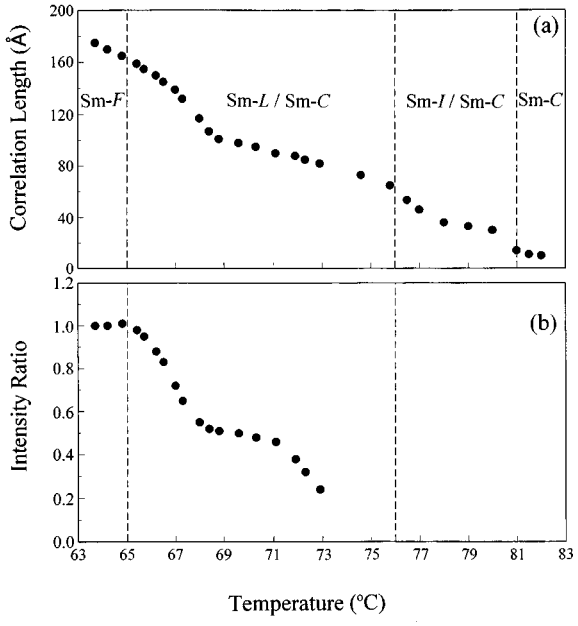

FIG. 7. Temperature dependence of (a) the positional correlation length of the surface hexatic phases and (b) the ratio of the integrated intensity of the surface Sm-L arc at 60° to that at 120° in Fig. 3 for a ten-layer FTE1 film.

this novel phenomenon occurs at about 68 °C. The presence of a structural transition at this temperature is indicated by the temperature behavior of both the positional correlation length and the tilt direction obtained from electron diffraction. Figure 7(a) shows the temperature dependence of the positional correlation length, which is obtained by fitting the diffraction intensity in the radial direction to either a Lorentzian function (for a Sm-*C*) or a square-root Lorentzian function (for a hexatic phase) [13,14]. Above 81 °C, the correlation length is measured in the Sm-*C* phase. From 81 °C to 65 °C, all the radial scans are taken midway across the strongest Sm-*L* arcs. Below 65 °C, the radial scans are taken across the Sm-*F* arcs. The correlation length of the surface hexatic phases increases progressively from 30 Å at 80 °C in the surface Sm-*I* phase to 175 Å at 63.7 °C in the Sm-*F* phase. The temperature dependence of the correlation length shows a distinct change in slope at about 68 °C, which corresponds to the temperature at which the stripes disappear and then reappear.

This behavior is echoed in the temperature dependence of the hexatic tilt direction. Figure 7(b) shows the relative intensities of two hexatic arcs versus temperature for a ten-layer film, computed by taking the ratio of the integrated χ-scan intensities of the arcs at 60° and 120° shown in Fig. 3. This ratio is sensitive to the azimuthal tilt direction relative to the hexatic bond axes. Below 65 °C, the entire film goes into the Sm-*F* phase, so the ratio is close to unity, as shown in Fig. 7(b). This ratio was not determined above 73 °C because the stripes in the Sm-*L* phase at higher temperatures are rather narrow, causing multidomain diffraction. It can be seen that the behavior of the intensity ratio in Fig. 7(b) shows a striking resemblance to that of the positional correlation length in Fig. 7(a), the temperature dependence of the intensity ratio also exhibiting a change in slope at about 68 °C. The intensity ratio at this temperature is about 0.5, indicating that the tilt direction of the surface Sm-*L* phase is midway between the Sm-*I* and Sm-*F* configurations. The reason for this apparent transition remains mysterious, but is likely related to a symmetry change. Above the transition (in region *B*), the Sm-*L* tilt $\hat{c}$ director points closer to the Sm-*I* (nearest-neighbor) direction, whereas below the transition (in region *A*), the $\hat{c}$ director is closer to the Sm-*F* (next-nearest-neighbor) direction. The momentary disappearance of the stripes at 68 °C may mean that the chiral Sm-L_1 and Sm-L_2 domains that comprise the stripes [7] are energetically equivalent at this temperature.

We are grateful to C. F. Chou for participation in the early phase of this work, R. Pindak for helpful discussions, and H. C. Box for technical assistance. The FTE1 material was kindly provided by U. Sohling and G. Decher. This work was supported by the National Science Foundation and the National Institutes of Health.

[1] S. B. Dierker and R. Pindak, Phys. Rev. Lett. **59**, 1002 (1987).
[2] E. B. Sirota, P. S. Pershan, L. B. Sorensen, and J. Collett, Phys. Rev. A **36**, 2890 (1987).
[3] G. S. Smith, E. B. Sirota, C. R. Safinya, and N. A. Clark, Phys. Rev. Lett. **60**, 813 (1988).
[4] G. S. Smith, E. B. Sirota, C. R. Safinya, R. J. Plano, and N. A. Clark, J. Chem. Phys. **92**, 4519 (1990).
[5] J. V. Selinger and D. R. Nelson, Phys. Rev. Lett. **61**, 416 (1988).
[6] J. V. Selinger and D. R. Nelson, Phys. Rev. A **39**, 3135 (1989).
[7] J. E. Maclennan and M. Seul, Phys. Rev. Lett. **69**, 2082 (1992).
[8] J. E. Maclennan, U. Sohling, N. A. Clark, and M. Seul, Phys. Rev. E **49**, 3207 (1994).
[9] C. Y. Chao, S. W. Hui, J. E. Maclennan, C. F. Chou, and J. T. Ho, Phys. Rev. Lett. **78**, 2581 (1997).
[10] M. Cheng, J. T. Ho, S. W. Hui, and R. Pindak, Phys. Rev. Lett. **59**, 1112 (1987).
[11] P. S. Pershan, *Structure of Liquid Crystal Phases* (World Scientific, Singapore, 1988).
[12] R. Pindak, M. Seul, and S. Heinekamp (unpublished).
[13] G. Aeppli and R. Bruinsma, Phys. Rev. Lett. **53**, 2133 (1984).
[14] S. C. Davey, J. Budai, J. W. Goodby, R. Pindak, and D. E. Moncton, Phys. Rev. Lett. **53**, 2129 (1984).